American Mineralogist, Volume 72, pages 515–527, 1987

Characterization and properties of a new synthetic silicate with highly charged mica-type layers

M. Gregorkiewitz, J. A. Rausell-Colom
Instituto de Ciencia de Materiales, Consejo Superior de Investigaciones Científicas, Serrano 115 bis, 28006 Madrid, Spain

Abstract

Colorless flakes of a new 2:1 layer silicate were obtained from reaction of augite in NaF-MgF_2 melts at approximately 900°C. Assuming a mica-type structure, electron-microprobe analyses yielded a mineralogical formula close to $Na_{4.0}(Mg_{6.0}Ti_{0.05})[Fe_{0.1}Al_{3.4}Si_{4.5}O_{20.7}F_{3.3}]$ with the layer charge of brittle micas and the unusually high number of four alkali ions in the interlayer region. Single-crystal X-ray and electron diffraction patterns give the cell dimensions $a\sqrt{3} = b = 9.24$ and $d_{001} = 9.81$ Å, characteristic for trioctahedral mica-type (2:1) layers. The infrared spectrum resembles that of fluorphlogopite and is consistent with the high Al-Si substitution in the tetrahedral sheet. Despite the high layer charge, the material readily hydrates to the first hydration state with $d_{001} = 12.18$ Å. Ion exchange is successful with K^+, yielding a stable hydrated phase of $d_{001} = 12.81$ Å, and with alkylammonium ions, yielding highly expanded two-layer complexes, but not with divalent inorganic cations. On the basis of $00l$ monodimensional structure refinements as well as a comparison of calculated and observed intensities on the $02l/0\bar{2}l$ and $11l/1\bar{1}l$ reciprocal lattice rows, and using the geometric relations for mica-type layers, models are proposed for the organization of cations and water in the interlayer space. The original anhydrous phase is characterized by a layer stacking with displacement in the (001) plane and Na deeply immersed in the ditrigonal holes above and below the central plane of the interlayer space. This arrangement provides four interlayer cation sites per unit cell, twice as many as for the mica structure, so that the unusually high number of interlayer cations may be accommodated. It is suggested that the same stacking might also occur in other mica-type silicates, which would have important implications for the interpretation of their crystal chemistry.

Introduction

Most 2:1 layer silicates (with a few exceptions such as sepiolite) contain mica-type layers forming distinct structural units that can separate along the stacking direction and adsorb matter between them whenever the cohesion forces across the interlayer space are small compared to those within the layer. The considerable differences in the properties of these silicates can be related to the chemical composition of the 2:1 layer, which determines such important parameters as the layer charge and its distribution, as well as the dimensions and the geometrical details for the different parts of the layer (see, e.g., Radoslovich and Norrish, 1962; Donnay et al., 1964).

The origin of the present work goes back to a series of earlier experiments that concerned the synthesis of mica-type silicates from fluoride melts and that were conducted with the aim of obtaining materials of definite layer charges. In the course of these experiments, a new layer silicate, hereafter informally referred to as Na-4-mica, was identified among the reaction products of augite in $NaMgF_3$ melt (Gregorkiewitz, 1972). Preliminary characterization of Na-4-mica led to the postulation of trioctahedral 2:1 layers, similar to those in fluorphlogopite, but with an unusually high Al-Si substitution in the tetrahedral sheet and charge compensation by three to four Na ions in the interlayer region (Gregorkiewitz et al., 1974).

Because no mica with more than two interlayer cations per unit cell had ever been observed, and because the existence of such a phase would be of considerable interest for mineralogy, further experiments were undertaken in order to substantiate the existence of Na-4-mica and thoroughly characterize both its structure and chemical properties. Most of these experiments were performed on a few milligrams of the original material (Gregorkiewitz, 1972), but at a later stage, the synthesis was improved by using pure oxides instead of augite, and additional experiments could be realized with the new material when greater quantities were required.

The present paper deals with the results of the mineralogical and chemical characterization of Na-4-mica; the relevance of this new phase to the crystal chemistry of micas is also discussed. Unless otherwise stated, the data in this paper refer to the original material. Data related to the material synthesized using pure oxides, as well as a more thorough study on the formation conditions of Na-4-mica, will be the subjects of a forthcoming paper.

0003–004X/87/0506–0515$02.00

TABLE 1. Analytical data for augite and Na-4-mica

		Na-4-mica and its derivatives**							
		Na phases, after leaching with water at 60°C for			Hydrated phase, after K exchange at 60°C for			Hydrated phase, after treatment with Mg and Sr	
	Augite*	0 h	12 h	60 h†	50 h	144 h	300 h	Bulk†	Rims†
					mass percent				
Na_2O	0.57	13.52	10.12	10.76	3.00	1.30	1.15	10.15	5.10
K_2O	0.29	0.11	0.07	0	11.32	15.06	14.47	—	—
CaO	22.63	0.32	0.05	0.03	0	0	0.02	0.20	0.46
SrO	—	—	—	—	—	—	—	0.55	6.36
MgO	14.29	26.08	25.16	26.07	24.71	25.45	24.88	29.37	26.02
MnO	0.14	0.02	0	—	0	0	0	—	—
TiO_2	0.30	0.33	0.43	0.31	0.37	0.22	0.40	(0.31)	(0.31)
FeO	3.03	1.00	1.30	—	0.98	1.18	1.24	—	—
Fe_2O_3	1.62	—	—	1.45	—	—	—	(1.34)	(1.34)
Al_2O_3	4.96	18.77	19.10	19.22	18.65	18.39	18.50	20.50	18.02
SiO_2	51.67	29.08	28.58	30.17	28.71	30.11	28.26	28.39	26.79
F	—	6.73	6.30	7.00	6.20	6.82	6.46	7.26	6.14
Cl	—	—	—	0.01	0.14	0.05	0.14	—	—
O = F††	—	−2.83	−2.65	−2.95	−2.61	−2.87	−2.72	−3.06	−2.59
Total	99.50	93.13	88.46‡	92.07	91.47	95.71	92.80	95.01	87.95
H_2O	0.53	(<9.6)	(9.6)	9.6§	(>7.8)	7.8§	7.8§	(9.6)	?
		Atoms per 24 negative ions (per 6 oxygens in the case of augite)							
Na	0.04	4.03	3.13	3.19	0.94	0.39	0.36	2.94	1.64
K	0.01	0.02	0.01	—	2.33	2.99	2.97	—	—
Ca	0.89	0.05	0.01	0.01	—	—	—	0.03	0.08
Sr	—	—	—	—	—	—	—	0.05	0.61
Mg	0.78	5.98	5.98	5.95	5.93	5.91	5.97	6.54	6.42
Ti	0.01	0.04	0.05	0.04	0.04	0.03	0.05	0.04	0.04
Fe^{2+}	0.09	—	—	—	—	—	—	—	—
Fe^{3+}	0.05	0.13	0.17	0.17	0.13	0.15	0.17	0.15	0.17
Al	0.22	3.40	3.59	3.47	3.54	3.38	3.51	3.61	3.51
Si	1.90	4.47	4.56	4.62	4.63	4.69	4.55	4.24	4.43
O	6	20.73	20.82	20.61	20.84	20.64	20.71	20.57	20.78
F	—	3.27	3.18	3.39	3.16	3.36	3.29	3.43	3.22
d_{001} (Å)	—	11–12.2	12.18	12.18	12.81:94% 12.18:6%	97% 3%	100% 0%	12.18	?
x, *y***	—	12, 2	7, 1	8, 1	4, 1	8, 1	8, 1	10, 1	7, 1

Note: — = not determined; ( ) = presumed on basis of other analyses.

* Wet-chemical analysis (Sinno, 1952) for augite crystals from 1944 eruption, collected near Boscotrecase, Mt. Vesuvius, Italy. Contains traces of Zr.

** Electron-microprobe analysis. Given figures correspond to average values from *x* points on *y* crystals. Wavelength-dispersive instrument, 15 kV, beam current 20 nA, beam diameter 20 μm, take-off angle 52.5°. Time of measurement 2 + 20 + 2 s for background + peak + background. Data reduction and correction procedures from Ziebold and Ogilvie (1964) and Albee and Ray (1970). Standards were albite BH3 for Na, microcline BH1 for K, olivine A1D for Mg, spessartine BH5 for Mn and Fe, ilmenite BH7 for Ti, garnet DD1 for Al, clinopyroxene A1P for Ca and Si, fluorite CaF_2 for F, and sodalite for Cl. Analyst: G. Vezzalini.

† Analyst: K. Norrish.

‡ Crystal of poorer quality.

†† $-\%F \times 15.9994/(2 \times 18.9984)$.

§ The value for H_2O was obtained by thermogravimetric analysis on samples from synthesis using pure oxides (Gregorkiewitz and Vezzalini, to be published).

RESULTS

Synthesis

The starting material for the synthesis of Na-4-mica was natural augite crystals from the 1944 eruption of Mt. Vesuvius, Italy. The composition of this mineral was studied by Sinno (1952, 1956), and a typical analysis is given in Table 1, showing about 5% Al-Si substitution in the tetrahedra of the pyroxene chain. For reaction, finely ground augite powder was placed in a Pt crucible together with a 1:1 mixture of NaF + MgF_2 (both puriss. Merck). The crucible was heated in an open furnace at 1080°C for approximately 4 h and then cooled down at a rate of 10°C/h until 850°C was reached.

The product was a heterogeneous mixture of crystalline phases, which could be separated under the petrographic microscope. Identification of the pure phases was made by X-ray diffraction using powder methods and a Gandolfi camera. The following phases were found: colorless, transparent cubes of neighbourite ($NaMgF_3$) as a major constituent of the mixture; transparent, light-yellow grains of chondrodite ($Mg_5(SiO_4)_2F_2$); dark hexagonal plates of hematite (Fe_2O_3); dark octahedra of magnetite (Fe_3O_4); and thin, colorless flakes of Na-4-mica, of hexagonal outline and about 0.1–2 mm in diameter. In total, about 20 mg of Na-4-mica were isolated for use in the characterization experiments. A repetition of the synthesis was successful, but Na-4-mica of this batch had a smaller crystal size and was only used to prove its identity with the former product.

Chemical composition

The results of electron microprobe analysis on various crystals of Na-4-mica are shown in Table 1. Analyses were performed on the original material (stored at ambient conditions after synthesis) and after increasing periods of leaching in water at 60°C.

There is a clear variation in the Na content, indicating 4 Na per unit cell in the original material and 3.2 Na after leaching. This phenomenon could be due to the dissolution of a second phase during leaching, but no variation was observed for the Na content in different flakes of the original material, and exactly 4 Na per unit cell were also found for a perfectly transparent dry crystal from a later synthesis (to be published) where impurities could be excluded beyond any doubt. Another explanation for the different Na content might be sought in the migration and/or evaporation of Na_2O under the electron beam, and its possible dependence on the hydration degree of the crystals. However, variations for the Na_2O percentage proved to be negligible within the time of data collection, and samples of the original material with different hydration degree gave exactly the same results. Finally, the lower Na content for the leached materials is also confirmed by comparison with the K-exchanged samples (Table 1), which show the same number of alkali ions (3.2–3.3 per unit cell), accompanied by a slight excess of multivalent cations which sum to 14.2–14.3 instead of 14.0 as required for full occupation of octahedral and tetrahedral positions.

According to these results, the oxide contents are converted to the mineralogical formulae in Table 2, assuming that in the leached materials interlayer alkali is partially replaced by multivalent cations. The latter could be supplied from dissolution of small quantities of Na-4-mica, whereas the 2:1 layer is apparently not affected by this process.

Because Na-4-mica hydrates in contact with water (see below), the hydration degree of the crystals to be used in the analysis was examined by X-ray diffraction and is reported in Table 1 by their interlayer spacings d_{001}. For the pure one-layer hydrates with d_{001} = 12.18 Å (Na phase) and 12.81 Å (K-exchanged phase), the water content was found to be 9.6 and 7.8% (Table 1), which gives totals, after summation to the dry constituents, of about 102%. Similar totals have also been found for the one-layer hydrate of Ba-Llano-vermiculite, which has a well-known hydration degree and was used as a test material under the same experimental conditions (to be published). Both Na-4-mica and Ba-Llano-vermiculite release the main part of their intracrystalline water at 80–90°C, and it can be assumed that water loss under the electron beam is responsible for the high totals.

Morphology and optics

The crystals have the shape of incomplete hexagons with some well-developed angles of 120°, and the outline of hexagons was frequently recognized both on the surface and in the interior of the flakes, similar to the phlogopite crystals described by Sunagawa and Tomura (1976). Sometimes, one or several regions with a spiral-like texture can be distinguished (Fig. 1A), and electron micrographs of the finely ground sample (Fig. 1B) reveal aggregates made up of oriented intergrowths of thin, hexagon-shaped single crystals. As a curiosity, a few flakes have chondrodite epitaxially grown on their surface, an observation that has also been made for synthetic fluorphlogopite (Köppen, 1950).

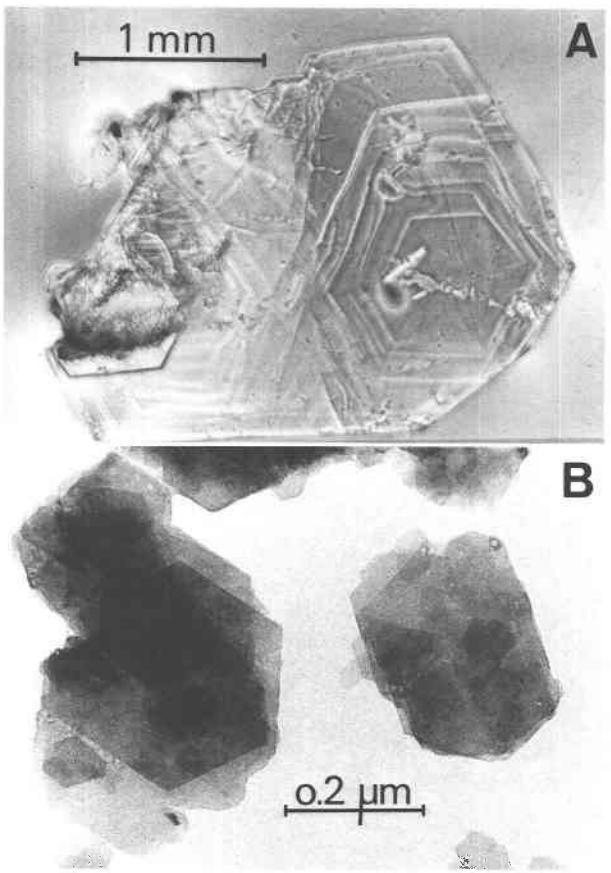

Fig. 1. (A) Microphotograph of Na-4-mica flake (transmitted light with phase contrast). (B) Transmission-electron micrograph of ground and H_2O-dispersed Na-4-mica.

Viewed perpendicular to the (001) plane under the polarizing microscope, most flakes appear isotropic, but in some instances, a very faint optical anisotropy is detected. In most of these cases, the extinction azimuth varies from place to place, and only a few samples show well-delimited regions with constant extinction azimuth, occasionally also in twin orientation to another region (rotation about **c*** by 60° or 120°). Thus, the optical behavior seems compatible with polytwinned growth of biaxial crystals of small $2V$, but uniaxial symmetry with internal stress cannot be excluded as an alternative.

Cell dimensions and diffraction symmetry

Single-crystal X-ray diffraction photographs were recorded for several flakes of original dry Na-4-mica and

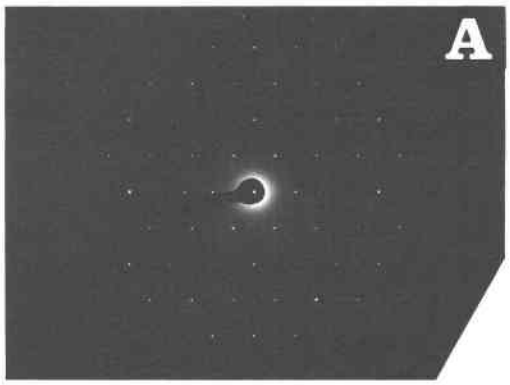

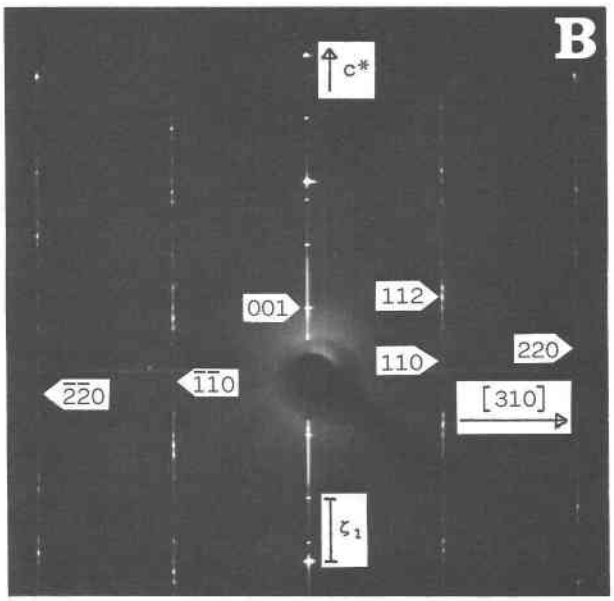

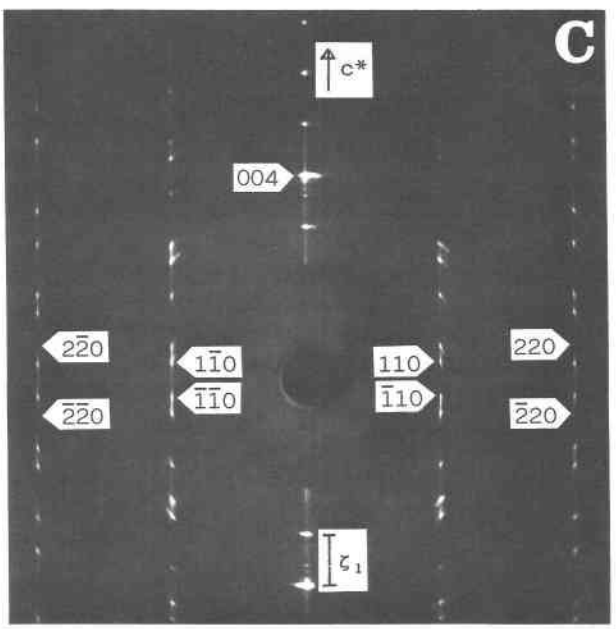

TABLE 2. Crystallographic data for Na-4-mica and its hydrated and K-exchanged derivatives

All phases: One-layer triclinic setting. Diffraction symmetry = $1C^*$. Modulated streaks $\parallel \mathbf{c}^*$ on hk with $k \neq 3n$.

9.81-Å dry phase

$Na_{4.0}(Mg_{6.0}Ti_{0.05})[Fe_{0.1}Al_{3.4}Si_{4.5}O_{20.7}F_{3.3}]$
molar mass: 857.8 g/mol. μ(Cu$K\alpha$, Mo$K\alpha$) = 94.6, 10.3 cm^{-1}.

a = 5.34(5) Å	α = 90.0(2)°	Z = 1
b = 9.24(5) Å	β = 100.3(2)°	ρ_{calc} = 2.943 g/cm^3
c = 9.97(6) Å	γ = 90.0(2)°	ρ_{obs} = 2.914 g/cm^3
d_{001} = 9.81(2) Å		$b/a = 0.999\sqrt{3}$
V = 484.0(5.3) Å^3		β_{calc} = 100.3(1)°

A two-layer monoclinic setting with c' = 19.70 Å and β' = 95.2° can also be established (see text).

12.18-Å hydrated phase

$Na_{3.2}(Mg_{5.95}Ti_{0.05}Fe_{0.15}Al_{0.10})[Al_{3.4}Si_{4.6}O_{20.7}F_{3.3}]\cdot 4.3H_2O$
molar mass: 924.0 g/mol. μ(Cu$K\alpha$, Mo$K\alpha$) = 79.9, 8.8 cm^{-1}.

a = 5.35(5) Å	α = 90.0(2)°	Z = 1
b = 9.24(5) Å	β = 98.5(2)°	ρ_{calc} = 2.55 g/cm^3
c = 12.32(6) Å	γ = 90.0(2)°	ρ_{obs} = 2.53 g/cm^3
d_{001} = 12.18(2) Å		$b/a = 0.977\sqrt{3}$
V = 602.1(6.6) Å^3		β_{calc} = 98.3(1)°

12.81-Å hydrated and K-exchanged phase

$K_{3.0}Na_{0.3}(Mg_{5.95}Ti_{0.05}Fe_{0.15}Al_{0.10})[Al_{3.4}Si_{4.6}O_{20.7}F_{3.3}]\cdot 4.0H_2O$
molar mass: 969.2 g/mol. μ(Cu$K\alpha$, Mo$K\alpha$) = 112.6, 12.4 cm^{-1}.

a = 5.39(5) Å	α = 90.0(2)°	Z = 1
b = 9.32(5) Å	β = 97.8(2)°	ρ_{calc} = 2.50 g/cm^3
c = 12.94(6) Å	γ = 90.0(2)°	ρ_{obs} = 2.50 g/cm^3
d_{001} = 12.81(2) Å		$b/a = 0.998\sqrt{3}$
V = 643.5(7.0) Å^3		β_{calc} = 98.0(1)°

$\beta_{calc} = \arctan(-3d_{001}/a)$. ρ_{obs} and β for the anhydrous phase were determined on crystals synthesized from pure oxides. The number of H_2O molecules was taken from the results of structural calculations (see text) and is similar to the values obtained by thermogravimetric analysis.

its one-layer hydrate, as well as for the hydrated K-exchanged derivative. Weissenberg and Buerger precession cameras were used, in most cases with Cu$K\alpha$ (λ = 1.5418 Å) radiation in order to achieve sufficient resolution. For all three phases, the unit-cell dimensions (Table 2) indicate a structure based on mica-type layers, with hexagonal dimensions $b = a\sqrt{3} \approx 9.3$ Å within the layer plane and a basal spacing d_{001} that increases from 9.81 to 12.81 Å as a function of the interlayer content. Both Weissenberg (a and b) and powder-diffractometer readings (d_{001}) were calibrated against external Si standards. Electron diffraction patterns (Fig. 2A) for selected crystallites of the hydrated Na-4-mica showed hexagonal symmetry within the layer plane and confirm the a and b dimensions obtained from X-ray experiments. As for phlogopite, the

←

Fig. 2. (A) Electron diffraction pattern for a single crystallite of hydrated Na-4-mica. (B) 0-level precession photograph for anhydrous Na-4-mica (a crystal synthesized from pure oxides was used) taken perpendicular to [$\bar{1}$10] when referred to the $2M_1$ individual (see text). (C) 0-level precession photograph for hydrated Na-4-mica taken perpendicular to the bisectrix between the **a** axes of the two individuals. Indices hhl correspond to individual 1 and $h\bar{h}l$ to individual 2 (see text).

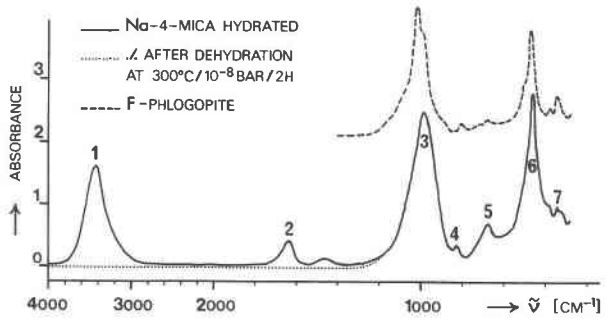

Fig. 3. Infrared absorption spectrum of Na-4-mica as compared with synthetic fluorphlogopite. 1:3435, 2:1638, 3:982, 4:828, 5:678, 6:462, 7:341 cm^{-1}.

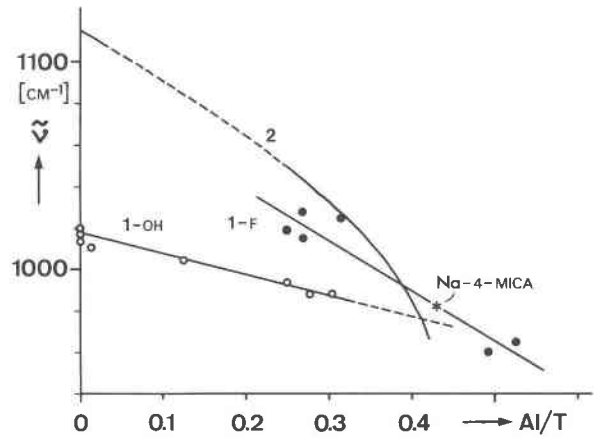

Fig. 4. Infrared absorption frequencies $\tilde{\nu}$(T–O) of mica-type silicates with trioctahedral layers $(Mg_6)[(Al,Si)_8O_{20}X_4]$ as function of the Al-Si substitution in the tetrahedral sheet. 1—curve for stretching vibration parallel to the layer plane (usually peak maximum) as obtained from published data (○, X = OH; ●, X = F); 2—curve for stretching vibration perpendicular to the layer plane (usually high-frequency shoulder) as given by Velde (1979).

9.3-Å period was found perpendicular to the edges of the hexagon that is defined by the basal face of the crystals.

Precession photographs taken at three different orientations of the same flake (perpendicular to **c***, **b** or ⟨310⟩, and **a** or ⟨110⟩) were combined to explore the intensity-weighted reciprocal lattice. In all cases, reflections with $k = 3n$ are sharp and distinct, whereas the remainder are diffuse and form streaks parallel to **c*** (Figs. 2B, 2C). The positions of the sharp reflections comply with the unit cells of Table 2, and their intensities are consistent with both monoclinic ($2/m$) and trigonal ($\bar{3}1m$) Laue symmetry. The diffuse reflections, on the other hand, show periods along **c*** that are smaller than $\zeta_1 = \lambda/d_{001}$ and cannot be explained by the simple unit cells of Table 2.

For dry Na-4-mica, the diffuse reflections show a period of $\frac{1}{6}\zeta_1$, with a characteristic sequence of intensities that repeats after every six periods (Fig. 2B), and their Laue symmetry is approximately $2/m$. Theoretical diffraction patterns were then constructed for the polytypes 1M, $2M_1$, $2M_2$, and 3T, as well as for all possible twins that can be generated by $n \cdot 60°$ or $n \cdot 120°$ rotations about **c*** between adjacent layers. Comparison of symmetry and absences (both systematical and the pseudo-absences corresponding to the "structural presence criteria" of Ross et al., 1966) pointed out that the diffraction pattern of dry Na-4-mica can be explained by the assumption of a $2M_1$ polytype, which has its layers at orientation $-60°$ and 60° (the angle gives the direction of the layer stagger as defined in Takeda, 1967), coexisting with equal amounts of a 1M polytype in two orientations ($-60°$ and 60°) at 120° between them. In addition, considerable disorder in the sequence of the individual polytypes must be assumed to account for the diffuse streaks on hk rows with $k \neq 3n$. Rotations of 60° as well as a $2M_2$ polytype can be excluded.

Other than for the dry phase, the diffuse reflections of hydrated Na-4-mica show a period of $\frac{1}{3}\zeta_1$ along **c*** (Fig. 2C). Using the same procedure as above, the diffraction patterns of several different flakes were analyzed. The degree of stacking disorder varies from flake to flake, but in all cases, absences are consistent with the assumption of a twin composed of two individuals with a 1M cell and rotation of 120° between them. However, intensities corresponding to a single individual clearly violate Laue symmetry $2/m$, so that a triclinic one-layer cell (1Tc) must be assumed in lieu of the usual monoclinic cell (1M) for mica structures.

The K-exchanged derivative of hydrated Na-4-mica shows a very similar diffraction pattern, but disorder as seen by the diffuse streaking along **c*** is much more pronounced than in the Na analogue.

Infrared spectra

The infrared spectrum of Na-4-mica is reported in Figure 3. For the hydrated form (d = 12.18 Å), there are strong peaks at 3435 and 1638 cm^{-1}, corresponding to the frequencies of H_2O stretching and bending, respectively. After release of the interlayer water by heating, both peaks disappear and the substance becomes completely transparent from 4000–1200 cm^{-1}. This is consistent with the analytical formula reported above and confirms that the 2:1 layers are free of OH groups.

The lower part of the spectrum (1200–300 cm^{-1}) corresponds to lattice vibrations $\tilde{\nu}$[(Si,Al)–O] and $\tilde{\nu}$(Mg–O) and, accordingly, resembles that of fluorphlogopite, which has a similar layer composition. A significant difference between the spectra is the shift of the (Si,Al)–O stretching band at $\tilde{\nu}$(T–O) ≈ 1000 cm^{-1} toward lower frequencies that may be accounted for by the increased Al-Si substitution in the tetrahedral sheet of Na-4-mica (Fig. 4).

Ion-exchange properties

To replace the interlayer Na cations by other monovalent or divalent cations, flakes were immersed in $0.5/m$ molar solutions of the corresponding chlorides MCl_m at 60°C for up to a 6-month period. Solutions were renewed daily, and checks were made in an X-ray diffractometer

TABLE 3. Ion-exchange properties of Na-4-mica

Na-4-mica (12.18 Å) $\xrightarrow[60°C,\ <6\ \text{months}]{0.5/m\ \text{molar}\ MCl_m}$ X

M^{m+} = Li^+, K^+, NH_4^+, Rb^+, Cs^+, Mg^{2+}, Ca^{2+}, Sr^{2+}, Ba^{2+}, $C_8H_{17}NH_3^+(OA^+)$, $C_{10}H_{21}NH_3^+(DA^+)$

X = 12.81-Å phase with M = K { completed after 7 d; 15 orders 00*l* observed

X = 29.4-Å phase with M = OA { completed after 7 d; 4 orders 00*l* observed

X = 33.4-Å phase with M = DA { completed after 7 d; 4 orders 00*l* observed

DA-exchanged phase (33.4 Å) $\xrightarrow[60°C,\ <1\ \text{yr}]{0.5/m\ \text{molar}\ MCl_m}$ X

M^{m+} = Li^+, Na^+, K^+, NH_4^+, Rb^+, Cs^+, Mg^{2+}, Ca^{2+}, Sr^{2+}, Ba^{2+}

X = 12.18-Å phase with M = Na { starts after 3 months; completed after 6 months; sharp 00*l* reflections

X = 12.81-Å phase with M = K { starts after 6 months; completed after 1 yr; diffuse 00*l* reflections

X = 11.4-Å phase? with M = NH_4 { completed after 3 months; very diffuse 00*l* reflections

for changes in d_{001}. The results are given in Table 3, from which it may be concluded that exchange occurs readily with K^+ and with the alkylammonium ions, whereas exchange with other monovalent and divalent cations does not seem to take place.

In order to ascertain this, chemical analyses of the product phases were made. Thus, for the K-exchanged (Table 1) and the alkylammonium-saturated material, electron-microprobe determinations of the alkali content showed that exchange is almost complete, with about 0.4 nonexchangeable Na per unit cell being retained in all cases. Furthermore, a flake treated with 0.25 *M* $SrCl_2$ for 6 months was washed overnight with water and analyzed for Sr. X-ray fluorescence spectroscopy indicated the absence of any significant amount of Sr in the bulk composition, whereas point determinations by electron-microprobe analysis on the same flake showed Sr substitution of about Sr/Na = 0.6/1.6 for spots at the rims, and practically zero Sr content in spots a few micrometers away toward the center (Table 1). This indicates that exchange has taken place at the edges of the flake, but has not proceeded further to completion.

In view of the apparent difficulties for cation diffusion, exchange reactions were also attempted in an indirect way, starting with the highly expanded 33.4-Å phase of the alkylammonium derivative (Table 3). Again, exchange was only successful with Na^+, restoring the 12.18-Å phase, with K^+, giving the 12.81-Å phase observed before by the direct exchange, and also with NH_4^+, giving very diffuse 00*l* reflections with d_{001} = 11.4 Å.

Hydration properties

The anhydrous 9.81-Å phase shows a remarkable affinity for water adsorption; it progressively hydrates even in moist air at normal ambient conditions to form a more stable phase of d_{001} = 12.18 Å, characterized by sharp 00*l* reflections observed to l = 18. In water, the observed transformations

$$9.81\ \text{Å} \underset{300°C,\ 1\ \text{mbar},\ 24\ \text{h}}{\overset{H_2O,\ 60°C,\ <1\ \text{d}}{\rightleftharpoons}} 12.18\ \text{Å}$$

$$\underset{0.1\ M\ \text{NaCl},\ 60°C,\ 1\ \text{d}}{\overset{H_2O,\ 60°C,\ >6\ \text{d}}{\rightleftharpoons}} 12.18\ \text{Å} + 13.60\ \text{Å}$$

indicate the slow development of a second hydrate with d_{001} = 13.60 Å that coexists within the same flake with the 12.18-Å hydrate and is characterized by somewhat broader 00*l* peaks observed to l = 8. From the variation of the intensities of the 12.18-Å and 13.60-Å peaks over time, a progressive transformation of the first hydrate into the second is inferred, but even after 1 yr of immersion in water, the 12.18-Å phase was still present in considerable proportion. On the contrary, transformation of the 13.60-Å phase into the 12.18-Å phase required only a brief treatment with 0.1 *M* NaCl solution. Heating at 100°C for 1 d under vacuum (1 mbar) led to an interstratified phase (broad 11.0-Å peak with nonrational orders), and heating at 300°C restored the anhydrous 9.81-Å phase. This phase remained stable up to 600°C, but it became amorphous after heating to 750–900°C for 1 d.

The K-saturated material also developed a second hydrate of 13.60 Å coexisting with the 12.81-Å phase,

$$12.81\ \text{Å} \underset{0.5\ M\ \text{KCl},\ 60°C,15\ \text{d}}{\overset{H_2O,\ 60°C,\ 5\ \text{d}}{\rightleftharpoons}} 12.81\ \text{Å} + 13.60\ \text{Å},$$

from which a single 12.81-Å phase could be restored after immersion in a more concentrated KCl-solution or by heating the crystals at 70°C for 15 min. Heating for 1 h at 130°C led to an interstratified phase with a diffuse 11.0-Å peak and nonrational orders. Heating above that temperature did not yield a crystalline, fully dehydrated phase as observed in the case with Na as interlayer cation.

One-dimensional electron-density projections

One-dimensional electron-density distributions along the normal to the silicate layers were calculated in an attempt to determine the height of the planes of interlayer cations and water molecules relative to the octahedral Mg plane.

Integrated intensities I_{00l} were recorded by $\omega/2\theta$ scan of oriented flakes on a powder diffractometer with Clemens-Brentano geometry. Both Ni-filtered Cu radiation and Zr-filtered Mo radiation were used, in connection with a scintillation counter. Applying corrections for background, Lorentz-polarization factor, and absorption for the case of symmetrical back-reflection from a thin flake that is small compared to the primary beam, the intensities were converted into observed structure amplitudes $F_o(00l)$. Eighteen $F_o(00l)$ with $I > 3\sigma I$ were obtained for the 12.18-Å hydrate of Na-4-mica using Mo$K\alpha$ radiation, and eleven for the dry 9.81-Å phase as well as fifteen for

the K-exchanged 12.81-Å hydrate using Cu$K\alpha$ radiation. Structure calculations for the 13.60-Å hydrates were not attempted because the observable data [six $F_o(00l)$ values with $l \leq 8$] were considered insufficient.

Calculated structure amplitudes $F_c(00l)$ were obtained using the scattering factors of the *International Tables for X-ray Crystallography* (1962) for the fully ionized atoms. The unit-cell content was slightly idealized ignoring the small quantities of Ti and Fe as well as protons of interlayer water. The one-layer distance d_{001} was chosen as unit period, assuming inversion points at the height of octahedral Mg ($z/d = 0$) and the center of the interlayer space ($z/d = ½$). Model coordinates z for the planes of atoms in the 2:1 layer were taken from published data for trioctahedral micas (e.g., Donnay et al., 1964) and were held constant throughout all calculations. Coordinates z of the interlayer cations and water molecules were found from difference Fourier syntheses, where $F_c^{2:1}(00l)$ were calculated for the 2:1 layer alone (Fig. 5). Refinement of these coordinates and their site-occupation factor was accomplished by iterative cycles of Fourier syntheses and structure-amplitude calculations, allowing for individual isotropic temperature factors at each plane. The error of the final models is expressed in terms of the R factor and can also be estimated from the deviation between the curves for $\rho_c(z)$ and $\rho_o(z)$ (Fig. 5).

9.81-Å dehydrated phase with Na. The electron-density projection for the dehydrated phase of Na-4-mica is shown in Figure 5a. The best agreement, $R = 0.03$, was obtained when 3.5 Na ions were placed at height 4.02 Å, far away from the center of the interlayer space at 4.905 Å.

12.18-Å hydrated phase with Na. For hydrated Na-4-mica (Fig. 5b), there are two peaks in the interlayer region, one plateau at 4–5 Å and one sharp peak at the central plane. Assuming all water at the central plane and postulating 3.2 Na ions per unit cell, the best agreement was obtained for the model in Figure 5b, which contains 4.3 H_2O at the central plane and Na at about 4.37 Å.

The fit between calculated and observed electron densities can be improved when the number of Na ions at 4–5 Å is reduced to about 1.6 per unit cell, but correlations between the Na site and an unavoidable ripple in the difference syntheses at 1.8 Å cast doubt on this result. The corresponding model also would significantly deviate from experimental data on chemical composition and density. In any case, the refinement indicates a high positional disorder at the Na site, and substitution of some interlayer water by Na cannot be excluded in view of the similarity of their scattering factors.

12.81-Å hydrated phase with K. In this phase, 4.0 H_2O molecules per unit cell were found, at height 6.09 Å, i.e., somewhat away from the central plane at 6.405 Å. The site-occupation factors of the interlayer cations refined to 2.7 K plus 0.6 Na ions per unit cell, in approximate agreement with the exchange degree of other crystals (cf. Table 1). The K ions were found at 4.575 Å and correspond to a clearly resolved peak in the Fourier synthesis, whereas the Na ions were placed arbitrarily at 4.02 Å for all calculations. This model is represented in Figure 5c and gives a significantly (Hamilton, 1965) better agreement than an alternative with Na at 4.37 Å.

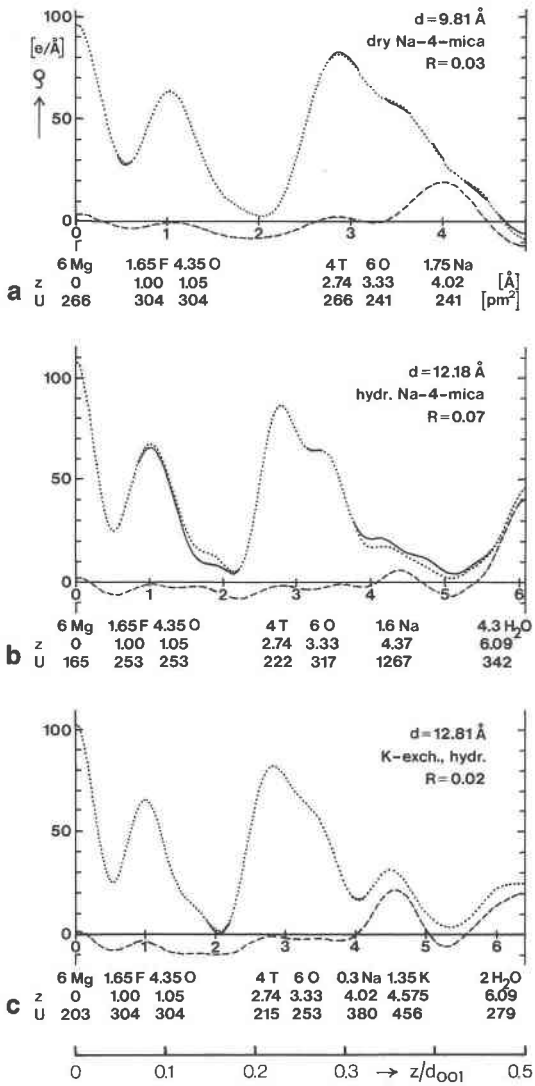

. . . . , $\rho_o(z) = [F(000) + 2\sum_l F_o(00l)\cos(2\pi lz/d)]/d$

——, $\rho_c(z) = [F(000) + 2\sum_l F_c(00l)\cos(2\pi lz/d)]/d$

– – –, $\Delta\rho(z) = \{2\sum_l [F_o(00l) - F_c^{2:1}(00l)]\cos(2\pi lz/d)\}/d$

Fig. 5. Monodimensional electron-density projections for Na-4-mica and its hydrated and K-exchanged derivatives. The isotropic temperature factor is $\exp(-8\pi^2 U \sin^2\theta/\lambda^2)$, where $U = \overline{u^2} = B/8\pi^2$ represents the mean square of the vibration amplitude. $F_c^{2:1}(00l)$ are the calculated structure amplitudes for the 2:1 layer alone, excluding interlayer material.

Intensity patterns on $02l/0\bar{2}l$ and $11l/1\bar{1}l$ reciprocal lattice rows

From the diffraction pattern of hydrated Na-4-mica, a one-layer polytype with triclinic symmetry was inferred (see above). The deviation from the monoclinic Laue class

TABLE 4. Observed and calculated structure amplitudes on selected reciprocal lattice rows, comparing different stacking models

	(a) 12.18-Å hydrated Na-4-mica						(b) 9.81-Å anhydrous Na-4-mica		
	*C*1*	obs.	*C*2/m*	obs	*C*1*		*C*2/*c**	obs.	*Cc**
l	02*l*	02*l*	0(±2)*l*	02$\bar{2}$*l*	02$\bar{2}$*l*	*l*	02*l*	02*l*	02*l*
0	18.2	19.4	37.7[A]	19.4	18.2	5	122.1[C]	57.4	61.4
1	47.2	47.2	19.2	38.7	28.7	7	11.7	124.3	119.8
2	3.3	18.4	62.0	45.8	56.8	9	92.7	44.7	45.2
3	77.7	49.1	34.3	43.9	44.6		11*l*	11*l*	11*l*
4	12.3	21.3	68.7	43.4	54.2	−12	39.0[D]	41.1	45.4
5	48.5	41.0	9.4	38.7	39.5	−10	71.7	21.3	17.3
6	17.9	16.1	33.6	16.1	14.5	−8	40.0	92.8	102.3
7	14.7	27.4	0.9	27.4	15.7	−6	66.7	79.2	100.8
	11*l*	11*l*	1(±1)*l*	1$\bar{1}$*l*	1$\bar{1}$*l*	−4	87.3	54.7	32.9
−7	8.4	16.5	13.6[B]	24.7	22.2	−2	5.6	88.2	66.8
−6	33.0	26.5	32.6	9.7	0.3	0	39.8	27.4	16.1
−5	40.3	33.7	16.0	44.9	56.5	2	26.1	89.8	74.9
−4	46.0	29.4	73.1	24.7	28.3	4	100.1	9.2	13.0
−3	63.5	56.0	5.1	52.8	68.7	6	29.4	82.2	121.4
−2	33.8	42.3	60.0	25.6	27.3	8	60.6	77.7	74.9
−1	30.3	48.0	9.3	54.6	39.7	10	66.5	10.7	8.4
0	35.2	53.1	27.9	8.9	6.9				
1	3.9	5.1	44.0	59.9	48.7				
2	72.6	58.1	38.9	33.4	33.0				
3	8.2	12.9	61.5	54.6	70.9				
4	63.6	50.9	43.5	22.9	19.4				
5	18.3	10.7	25.8	37.9	44.6				
6	21.8	23.6	24.1	10.5	2.8				
7	5.2	17.2	8.0	17.6	13.3				
Residuals			0.72		0.26†		0.82		0.19

Note: Superior letters indicate calculated *F* values scaled with factor (A) 1.030, (B) 0.985, (C) 1.122, or (D) 0.903.

* Models: *C*2/*m* denotes the 1M polytype, where the *inter*layer stacking vector $-a/3$ is given by the *intra*layer stagger; *C*1 denotes a triclinic one-layer polytype 1Tc, where the *inter*layer stacking vector is $-a/3 - b/3$ when referred to the ideal monoclinic single layer. *C*2/*c* denotes the $2M_1$ polytype; *Cc* denotes a 2M polytype with alternating *inter*layer stacking vectors $-a/3 - b/3$ and $-a/3 + b/3$. Thermal-vibration amplitudes (defined in Fig. 5) were 253 pm² for O and F, 101 pm² for Mg and Al/Si, and 380 pm² for interlayer Na.

† Includes both *hkl* and *hk̄l*.

$2/m$ is strong, but it concerns only reflections with $k \neq 3n$. This behavior suggests a layer stacking with translation of $\pm\mathbf{b}/3$ between adjacent mica-type layers. In order to prove this hypothesis, observed and calculated structure amplitudes on the reciprocal lattice rows $02l/02\bar{2}l$ and $11l/1\bar{1}l$ were compared for models with and without this translation.

Observed structure amplitudes were obtained from reflection intensities of $0kl$ and $1kl$ precession photographs (see, e.g., Fig. 2C) for several different crystals. Ni-filtered Cu radiation was used, and the visually estimated intensities were corrected for background and Lorentz-polarization factor. Calculated structure amplitudes correspond to the same unit-cell content and z coordinates as in the preceding section (see Fig. 5b), except that interlayer H_2O was omitted. Atomic x, y coordinates within a single layer were obtained from the layer composition and the b dimension using the geometrical relations for mica-type layers (Radoslovich and Norrish, 1962; Donnay et al., 1964), the ionic radii from Shannon and Prewitt (1969, 1970), and T–O distances from Zvyagin and Soboleva (1979). Temperature factors were given arbitrary values that are typical for mica structures (Table 4).

The resulting intensity patterns are summarized in Table 4a and show that the proposed stacking mode with translation along $\pm\mathbf{b}/3$ accounts excellently for the observed deviation from monoclinic symmetry.

Similar calculations were also performed for the anhydrous Na-4-mica. In this case, a stacking with translation along $\pm\mathbf{b}/3$ gives no deviations from the monoclinic Laue symmetry of the $2M_1$ cell, but the different stacking modes can be recognized on the basis of typical intensity patterns along suitable hk rows. Calculated structure amplitudes showed that differences occur on the $02l$ row for $l = 2n + 1$ and on the $11l$ row for $l = 2n$. Fortunately, these are just the reflections that were free from any twin contribution (cf. Fig. 2B) so a comparison with the observed structure amplitudes could be established (Table 4b). As for the hydrated phase, the experimental data suggest a stacking mode with translation along $\pm\mathbf{b}/3$ between adjacent layers.

DISCUSSION

Although there is a close metric relationship between mica ($a = 5.3$, $b = 9.2$, $d_{001} = 9.6$ Å) and augite (a pyroxene with $a = 5.3$, $b = 9.0$, $d_{001} = 9.5$ Å, in the setting referred to the mica structure), the formation of Na-4-mica is probably not a topotactic reaction because the tetrahedral Al content in the mica ($Al_t = 0.43$) is very different from that in augite ($Al_t = 0.05$), and the latter must have lost a considerable amount of Si for the formation of chondrodite. Na-4-mica is therefore regarded as a reorganization product of augite in $NaMgF_3$ melts, in agreement with other results supporting a predomi-

nantly reconstructive mechanism for silicate syntheses in fluoride melts (Gregorkiewitz, 1972).

Composition and classification

By its composition, Na-4-mica belongs to the series of trioctahedral mica-type silicates (full occupancy of the cation sites in the octahedral sheet). This is also supported by the cell dimensions in the layer plane with $b = a\sqrt{3} = 9.24(5)$ Å, which compares well with the expected value for the present composition, $b = 9.182(53)$ Å, calculated by the formula for trioctahedral micas from Veitch and Radoslovich (1963). The octahedral sheet of Na-4-mica contains Mg almost exclusively, as in the case of phlogopite, but the considerably higher Al substitution for Si in the tetrahedral sheet leads to the layer charge of brittle micas ($z = -4$). The typical brittle micas are clintonite (trioctahedral) and margarite (dioctahedral), both with Ca as interlayer cation, and only a few compounds with $z > 2$ and interlayer cations other than Ca have been reported as follows: the solid solution CaAl → NaSi in margarite (Afanasev and Aidinyan, 1952; Velde, 1971, 1980; Franz et al., 1977) and, in the trioctahedral series, two Ba-K micas (Kato et al., 1979; Guggenheim and Kato, 1984) and two Ba micas (McCauley and Newnham, 1973; Giuseppetti and Tadini, 1972).

Unlike these materials, Na-4-mica contains >2 interlayer cations per unit cell, and it easily hydrates despite the high layer charge. These observations are surprising. However, they can be consistently explained as will be seen in the following.

Proposed interlayer structures

9.81-Å dry phase. The dehydrated and the originally obtained anhydrous phase of Na-4-mica have the layer spacing characteristic for a dense stacking, where adjacent layers are almost in contact. The classical model for dense stacking is given by the mica structures in which the silicate nets of adjacent layers project almost on top of one another. In this stacking mode, the holes in the layer surface, defined by the hexamer silicate rings, superimpose face to face, and the center of the resulting cavity (two per unit cell) is occupied by the interlayer cation. This configuration cannot be assumed for Na-4-mica because the Na ions are found far away from the central plane of the interlayer space (see Fig. 5a). Also, their high number excludes a face-to-face stacking if double occupation of the cavities, with unrealistically short distances (d_{Na-Na} = 5.79–4.02 = 1.77 Å), is to be avoided.

The only alternative is a model where adjacent layers are displaced parallel to the layer plane (cf. Fig. 6) so that every hole becomes an independent cavity above and below the central plane between the layers and up to four cation sites per unit cell are allowed for. The resulting coordination for the interlayer cations may be estimated from the one-dimensional structure data and the layer geometry as derived from the b axis and chemical composition. Based on the usual relations (see above), one obtains a ditrigonal rotation of $\alpha = 14.2°$ for the hexamer

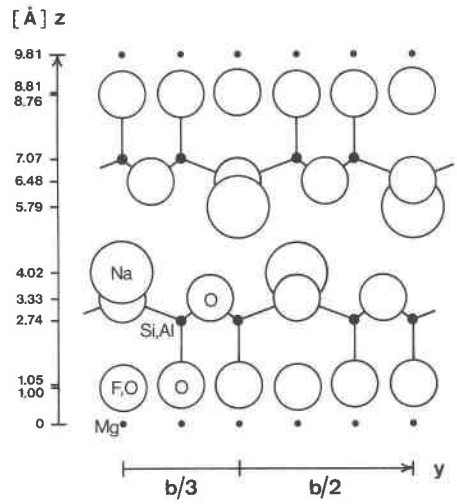

Fig. 6. Proposed model for anhydrous Na-4-mica as projected on plane perpendicular to **a**. The displacement of the upper layer with respect to the lower one is +**b**/3.

silicate rings, which is low compared to paragonite or clintonite (with $16 < \alpha < 19°$ and $\alpha = 23°$, respectively; see Bailey, 1984) and means a relatively open conformation for small interlayer cations. This allows Na to sink deeply into the hole (Fig. 6) where it is coordinated to three near (inner) and three far (outer) basal oxygens plus one F from the octahedral sheet, at distances $d_{Na-O_{in}} = 2.38$ Å (the sum of the ionic radii), $d_{Na-O_{out}} = 3.13$ Å, and $d_{Na-F} = 3.02$ Å. The bond Na–O_{in} makes an angle of 17° with the layer plane and meets well with the lone pair of O_{in} at about 7° elevation from the layer plane. The angle O_{in}–Na–O_{in} is 112° and suggests that the three inner oxygens provide the base of a tetrahedron (NaO_4) whose apex is an oxygen O′ from the adjacent layer. The shortest possible distance $d_{Na-O'} = 6.48–4.02 = 2.46$ Å is obtained when O′ lies vertically above Na, corresponding to a displacement of the upper layer by 2.28 Å along −**a**. From bond distances alone, this configuration seems acceptable, but it implies short repulsive distances $d_{Na-Na} = 2.88$ and 3.55 Å, and a poor shielding of Na by the upper layer because the four next-nearest oxygens are far away at $d_{Na-O'} = 3.68$ Å. An alternative model implies displacement along ±**b**/3, which is also supported from the intensity pattern on 02l and 11l rows (Table 4b). It provides the maximum distance between the interlayer cations, $d_{Na-Na} = 3.55$ Å, and a reasonably good shielding of Na by three oxygens from the upper layer, but the Na–O′ distances (2.92 Å) are now excessive.

Thus, whatever the actual displacement is, the stacking mode of anhydrous Na-4-mica always implies some defect in the electrostatic valence balance of the interlayer region that is consistent with the observed instability toward the hydrated phase.

A stacking mode with displacement in (001) and with Na being deeply immersed in the ditrigonal holes above and below the central plane was also postulated by

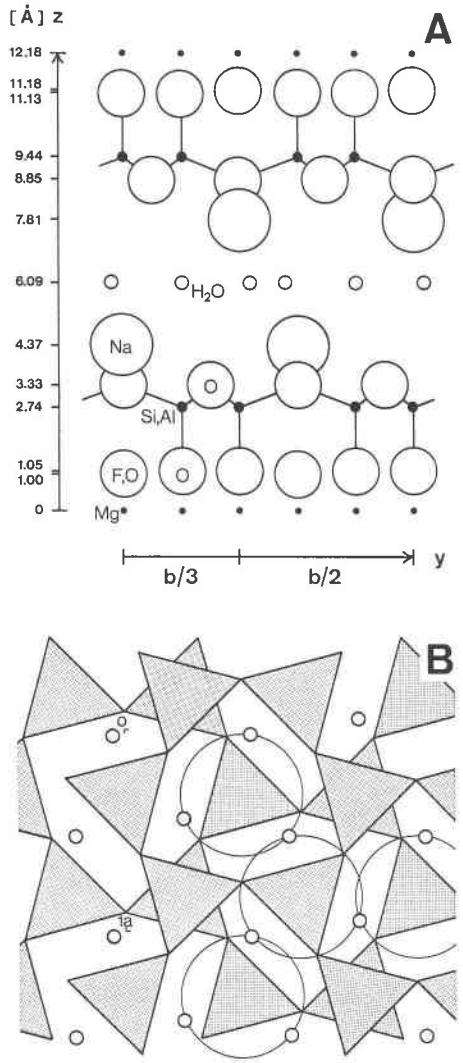

Fig. 7. Proposed model for hydrated Na-4-mica. The displacement between adjacent layers is +**b**/3. The model shows 4 Na and 6 H_2O sites per unit cell. Only 3.2 and 4.3 are actually occupied. (A) Projection on plane perpendicular to **a**; (B) projection on (001).

Pedro (1974), Méring (1975), and Besson (1980) for the anhydrous phases of Na-montmorillonite ($Na_{0.7}(Al_{3.3}Mg_{0.7})[Si_8O_{20}(OH)_4]$) and Na-beidellite ($Na_{1.1}(Al_4)[Al_{1.1}Si_{6.9}O_{20}(OH)_4]$). The OH dipoles of these compounds lie almost parallel to the layer plane, as opposed to those in trioctahedral compounds that point vertically upward toward the center of the hole. Hence, in dioctahedral compositions, the descent of Na into the hole is not hindered by repulsive interactions. The same argument holds also for trioctahedral layers with F in lieu of OH, so that the asymmetric configuration of Na in Na-4-mica, rather than being a unique case due to the high number of interlayer cations, appears to follow a general trend for compounds with displaced layer stacking and where the descent of cations is not hindered by vertical OH dipoles.

12.18-Å hydrated phase with Na. The layer spacing of this phase is characteristic for a stacking with one sheet of water molecules between adjacent layers. According to the results in Figure 5b, Na is bound to the ditrigonal holes on the layer surface nearly at the same position as in the anhydrous phase, but its coordination sphere is now completed by water molecules from the central plane. The coordination to the layer is fixed with a Na–O_{in} distance of 2.50 Å from the three inner basal oxygens, whereas the water molecules can in principle move freely on the central plane (which lies at 2.76 Å from the basal oxygens) as long as the minimum distance to Na is respected. Assuming equilibrium distances of $d_{Na-OH_2} = 2.38$ Å, the H_2O molecules lie on a circle with a radius of 1.64 Å centered above the Na ion (Fig. 7). There may be ≤ 3 H_2O molecules on this circle, which gives a distorted octahedron of $NaO_3(OH_2)_3$ with O–Na–O = 104° and H_2O–Na–OH_2 = 74°. The actual number of water molecules per Na ion can be estimated by a simple consideration as follows: if every H_2O is allowed to be shared by two cations, the number of H_2O per unit cell is given by

$$n_{H_2O} = \Sigma\, n_i w_i/2 \qquad (1)$$

where n_i = number of cations of species i per unit cell and w_i = number of H_2O for each ion of species i. Introducing the experimental values from chemical analysis (Table 1) and one-dimensional structure refinement (Fig. 5b), one finds $w_{Na} = 2n_{H_2O}/n_{Na} = 2 \cdot 4.3/3.2 \approx 2.7$ water molecules for each Na ion, suggesting that the actual coordination number of Na lies between 5 and 6.

There are few comparative data on the structure of mica-type silicates in a first hydration state and with Na as interlayer cation. They show that in vermiculites (Le Renard and Mamy, 1971; de la Calle, pers. comm.) and in saponites and beidellite (Suquet et al., 1980), both H_2O and Na lie close to the central plane at heights from 5.60 to 6.20 Å, whereas montmorillonite (Pedro, 1974) might have its Na immersed in the hole at $z \approx 4.25$ Å. Na-4-mica differs from vermiculite and saponite in that it lacks vertical OH dipoles that destabilize the in-hole position of interlayer cations. This fact, together with the high negative charge on the tetrahedral sheet, is likely to favor the in-hole position that provides also for maximum distance between interlayer cations, a parameter that should be important for compositions with more than two interlayer cations per unit cell. This last aspect is particularly interesting because even an alternative model (see discussion of Fig. 5b), with Na at the central plane, requires an important fraction of Na (≈ 1.6 per unit cell) at the in-hole position.

12.81-Å hydrated phase with K. The layer spacing of this phase agrees well with published values for the first hydration states in K-exchanged saponites and beidellites (12.60–12.70 Å, Suquet et al., 1975). According to the results in Figure 5c, the K ions are found in the ditrigonal holes, and the water molecules are on either side of the

central plane (Fig. 8) at the same height as in the Na analogue. This means that H_2O should have the same position in both phases, probably anchored by a H bond above a basal oxygen ($\Delta z = 2.76$ Å). In the K phase, H_2O is anchored alternatively to the lower or the upper layer, but the two positions differ little in height ($\Delta z = 0.63$ Å) and constitute still a unique, although somewhat puckered, water layer.

On the basis of these data, the interlayer organization should be as follows. The ditrigonal rotation angle is $\alpha = 12.1°$, somewhat less than in the Na phase. K is coordinated to three inner basal oxygens at a remarkably short distance $d_{K-O} = 2.66$ Å, the K–O bond making an angle of 28° with the layer plane. Together with three outer basal oxygens at 3.27 Å, they provide a reasonable coordination shell from one side which has to be completed by water molecules from the interlayer region. Assuming $d_{K-OH_2} = 2.74$ Å and considering a particular K ion, the water molecules associated to its own layer (H_2O) lie on a circle above K with $r = 2.28$ Å and the water molecules of the adjacent layer (H_2O') on a circle with $r = 1.71$ Å (Fig. 8B). There may be ≤ 4 water molecules on the first circle and ≤ 3 on the second, with angles between the layer plane and the K–OH_2 bond of 34° and 52°, respectively. The actual number of water ligands is (Eq. 1) $2 \cdot 4/2.7 \approx 3$ for every K ion, suggesting the octahedral coordination polyhedra $KO_3(OH_2)_3$ and $KO_3(O'H_2)_3$.

In view of these considerations, a face-to-face stacking of adjacent layers is improbable; it would imply a relatively short distance $d_{K-K} = 3.66$ Å, and in addition it would preclude water molecules from lying on the small circles and, hence, being shared by two neighboring K ions. The result would be an unrealistically low number of $4/2.7 \approx 1.5$ water molecules per K. A more realistic stacking mode is shown in Figure 8B. This model has a translation of **b**/3 between adjacent layers and contains six H_2O sites per unit cell, statistically associated either to the upper or the lower layer. In both positions, H_2O is bound simultaneously to a K of the upper and the lower layer so that, on an average, all K ions have the same coordination polyhedron, intermediate between $KO_3(OH_2)_3$ and $KO_3(O'H_2)_3$. The second polyhedron fixes the layer spacing, a result that is particularly useful for the understanding of the interlayer arrangement in other K-saturated one-layer hydrates (e.g., K-saponite). Since all these compounds have their K located in the hole, the constant value of their layer spacings at $d_{001} = 12.6$–12.7 Å suggests that it is determined by the same polyhedra $KO_3(O'H_2)_3$ and, hence, by a structure as in the present material regardless of what the actual layer charge is.

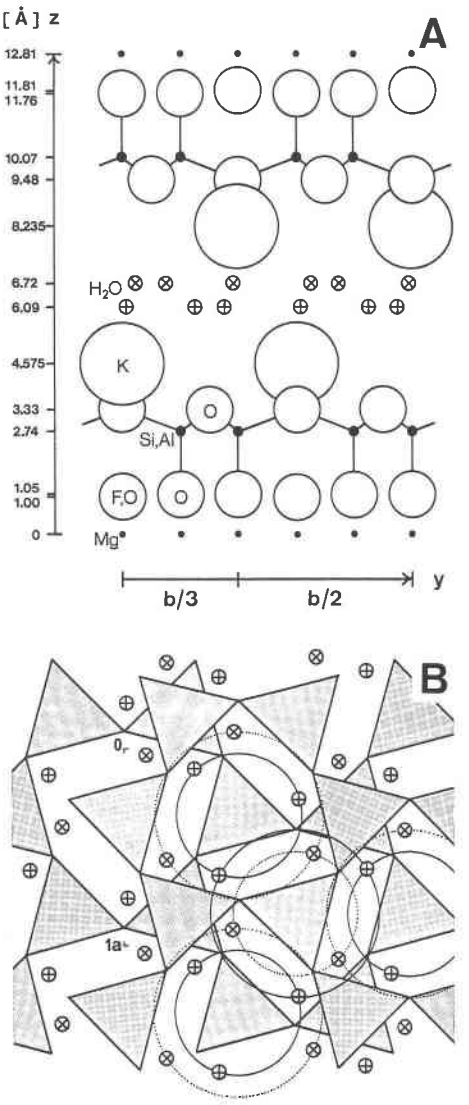

Fig. 8. Proposed model for the K-exchanged phase. The displacement +**b**/3 of the upper layer was inferred from crystallochemical reasons and is compatible with the diffraction aspect. The nonexchangeable ~0.4 Na at $z = 4.02$ Å are omitted for clarity. The H_2O sites at 6.09 Å (⊕) and 6.72 Å (⊗) are to be occupied alternatively. Thus, the model offers 4 K and 6 H_2O sites per unit cell, with an actual occupation of about ⅔ for both. (A) Projection on plane perpendicular to **a**; (B) projection on (001). Full circles: projected bond distance d_{K-OH_2} to H_2O at 6.09 Å; dotted circles: projected bond distance d_{K-OH_2} to H_2O at 6.72 Å.

Hydration and cation-exchange properties

It is known from other mica-type silicates (e.g., vermiculite, montmorillonite, etc.), that the hydrated phases collapse to stable anhydrous phases when interlayer Na is replaced by the larger K ions. Na-4-mica does not follow this reaction scheme, but the K-exchanged material is preserved in its hydrated state with $d_{001} = 12.81$ Å. Even by heating, the corresponding dehydrated state cannot be obtained. This is a logical consequence of the high number of interlayer cations. Even the most favorable model for an anhydrous phase with more than two K per unit cell implies unrealistically short repulsive distances of $d_{K-K} \approx 3.31$ Å and a poor shielding of K from the adjacent layer (K cannot sink in the hole as deeply as Na!).

The collapse of hydrated Na-4-mica to a stable anhy-

drous phase can be expected, however, if the replacement of Na with a larger ion implies at the same time the numerical reduction of the interlayer cations from 3.2 to 2 per unit cell. This requirement is met by Sr, and the observed exchange at the rims of the crystals, with an approximate composition of 1.6 Na + 0.6 Sr $\approx$ 2 ions per unit cell, suggests indeed the formation of a tightly closed phase on the borders which prevents the reaction from proceeding to the interior of the crystals. A similar sealing mechanism has been claimed for natural dry Na phlogopite (Schreyer et al., 1980) which is bordered by stable K phlogopite so that the usually observed hydration of Na phlogopite cannot take place.

Another interesting feature of Na-4-mica is the stability of its one-layer hydrate against further water uptake, which is in contrast to the easy transition to the two-layer hydrate of comparable materials. At first glance, this behavior may be explained by the usual argument that hydration capacity decreases as layer charge increases, but another explanation seems possible as well. In the two-layer hydrates, all cations are at the central plane between the water layers (e.g., Shirozu and Bailey, 1966). As there are two cation positions per unit cell, the compounds with ≤ 2 cations (saponites, vermiculites, etc.) can form the two-layer hydrate, whereas Na-4-mica, with its excess interlayer cations, cannot. This picture could also explain the replacement of interlayer Na by multivalent cations (see discussion concerning Table 1) and the appearance of the 13.60-Å phase that are observed after leaching in H_2O. It seems that a lower number of small interlayer cations favors the formation of a two-layer hydrate, whereas treatment with NaCl or KCl solutions restores the pure one-layer phases.

Implications

The most outstanding feature of Na-4-mica is the high layer charge and its compensation by more than two interlayer cations per unit cell, which imposes a layer stacking with displacement in the (001) plane and up to four sites for interlayer cations, even in the anhydrous state. This structure differs essentially from the classical dense stacking with face-to-face configuration of the ditrigonal holes; consequently, it is not subject to many of the crystallochemical constraints for the mica group that are derived from geometrical relations implying the classical model. It seems therefore necessary to redefine the validity of the generally accepted concepts on the structure of micas as will be illustrated in the following examples.

Trioctahedral Na micas have been postulated to be unstable (Radoslovich, 1963a, 1963b). Strictly speaking, however, this statement refers only to the face-to-face stacking, whereas for a displaced stacking, there may be stable phases with Na associated with trioctahedral layers. The Na phlogopite reported by Carman (1974) seems a possible candidate.

The control of the tetrahedral Al-Si substitution by the interlayer cation must necessarily depend on the stacking mode with its particular cation position so that the limits of the degree of Al-Si substitution may be different from those predicted by Radoslovich (1963a, 1963b) and Hazen and Wones (1978).

Structural comparisons can be misleading if the stacking mode is not taken in consideration. An illustrative example for this is given in the plot of d_{001} in phlogopites against the radius of the interlayer cation (Hazen and Wones, 1972) where the Na member falls outside the expected curve. In fact, the chosen compound is likely to have a displaced stacking, and replacing it by Na eastonite (Franz and Althaus, 1976; Keusen and Peters, 1980) yields a fairly straight line.

Finally, the existence of a stacking mode with more than two cation sites per unit cell calls for a new interpretation of the many mineral analyses with excess alkali (e.g., Koch, 1934; Sanero, 1940; Arkhipenko et al., 1964; Wearing, 1984). The corresponding materials might indeed contain regions with stacking as in Na-4-mica, and in order to verify this they should be inspected for their structure and possible displacements in the (001) plane. In some cases, excess Na has tentatively been placed in vacancies of the octahedral sheet (Arkhipenko et al., 1964). However, the probability of such a model is low because up to now, there are no indications for Na in this position except perhaps for very low quantities as in the case reported by Hazen et al. (1981).

Acknowledgments

The authors are indebted to Dr. G. Vezzalini, Istituto di Mineralogia, Università di Modena, Italy, and Dr. K. Norrish, Soils Division, CSIRO, Adelaide, Australia, who kindly made the electron-microprobe analyses. Fruitful discussions with Dr. J. F. Alcover, Centre de Recherche sur les Solides à Organisation Cristalline Imparfaite, CNRS, Orléans, France, are gratefully acknowledged. Thanks are also due to Dr. J. M. Serratosa, Instituto de Ciencia de Materiales, CSIC, Madrid, for critical reviewing of the manuscript.

Financial support from Bundesgesetz zur Graduiertenförderung, FRG, and Fundación Ramón Areces, Madrid, is gratefully acknowledged.

References

Afanasev, G.D., and Aidinyan, N.Kh. (1952) On sodium margarite from northern Kaukasus. Izvestiya Akademii Nauk SSSR, Seriya Geologicheskaya, 2, 138–140 (in Russian).

Albee, A.L., and Ray, L. (1970) Correction methods for electron microanalysis of silicates, oxides, carbonates, phosphates, and sulfates. Analytical Chemistry, 42, 1408–1414.

Arkhipenko, D.K., Bobr-Sergeev, A.A., Grigoreva, T.N., and Kovaleva, L.T. (1964) On the possibility of occupation of the octahedral positions in micas with monovalent sodium cations. Doklady Akademii Nauk SSSR, 160, 2, 429–431 (in Russian).

Bailey, S.W., Ed. (1984) Micas. Mineralogical Society of America, Reviews in Mineralogy, 13, 584 p.

Besson, G. (1980) Structures des smectites dioctaédriques. Paramètres conditionnant les fautes d'empilement des feuillets. Thèse de docteur, Université d'Orléans, France, 160 p.

Carman, J.H. (1974) Synthetic sodium phlogopite and its two hydrates: Stabilities, properties, and mineralogical implications. American Mineralogist, 59, 261–273.

Donnay, G., Donnay, J.D.H., and Takeda, H. (1964) Trioctahedral one-layer micas. II. Prediction of the structure from composition and cell dimensions. Acta Crystallographica, 17, 1374–1381.

Franz, G., and Althaus, E. (1976) Experimental investigation on the formation of solid solutions in sodium-aluminium-magnesium micas. Neues Jahrbuch für Mineralogie, Abhandlungen, 126, 233–253.

Franz, G., Hinrichsen, T., and Wannemascher, E. (1977) Determination of the miscibility gap in the solid solution series paragonite-margarite by means of infrared spectroscopy. Contributions to Mineralogy and Petrology, 59, 307–316.

Giuseppetti, G., and Tadini, C. (1972) The crystal structure of 2O brittle mica: Anandite. Tschermaks Mineralogische und Petrographische Mitteilungen, 18, 169–184.

Gregorkiewitz, M. (1972) Zur darstellung von tektosilicaten in salzschmelzen. Diplomarbeit, Universität München, 63 p.

Gregorkiewitz, M., Alcover, J.F., Rausell-Colom, J.A., and Serratosa, J.M. (1974) Characterization and properties of a high charge synthetic fluorphyllosilicate. 2ème Réunion des Groupes Européens d'Argiles, Strasbourg, 64.

Guggenheim, S., and Kato, T. (1984) Kinoshitalite and Mn phlogopites: Trial refinements in subgroup symmetry and further refinement in ideal symmetry. Mineralogical Journal Japan, 12, 1–5.

Hamilton, W.C. (1965) Significance tests on the crystallographic R-factor. Acta Crystallographica, 18, 502–510.

Hazen, R.M., and Wones, D.R. (1972) The effect of cation substitutions on the physical properties of trioctahedral micas. American Mineralogist, 57, 103–129.

——— (1978) Predicted and observed compositional limits of trioctahedral micas. American Mineralogist, 63, 885–892.

Hazen, R.M., Finger, L.W., and Velde, D. (1981) Crystal structure of a silica- and alkali-rich trioctahedral mica. American Mineralogist, 66, 586–591.

International tables for X-ray crystallography, volume III. (1962) C.H. Macgillavry, G.D. Rieck, Eds. Kynoch, Birmingham, 362 p.

Kato, T., Miura, Y., Yoshii, M., and Maeda, K. (1979) The crystal structures of 1M-kinoshitalite, a new barium brittle mica, and 1M-manganese trioctahedral micas. Mineralogical Journal Japan, 9, 392–408.

Keusen, H.R., and Peters, T. (1980) Preiswerkite, an Al-rich trioctahedral sodium mica from the Geisspfad ultramafic complex (Penninic Alps). American Mineralogist, 65, 1134–1137.

Koch, G. (1934–1935) Chemische und physikalisch-optische zusammenhänge der sprödglimmergruppe. Chemie der Erde, 9, 453–463.

Köppen, N. (1950) Gesetzmässige verwachsung von synthetischem phlogopit mit mineralien der humitgruppe. Neues Jahrbuch für Mineralogie, Geologie, und Paläontologie, Abhandlungen, A, 80, 343–374.

Le Renard, J., and Mamy, J. (1971) Etude de la structure des phases hydratées des phlogopites altérées par des projections de Fourier monodimensionnelles. Bulletin du Groupe français des Argiles, 23, 119–127.

McCauley, J.W., and Newnham, R.E. (1973) Structure refinement of a barium mica. Zeitschrift für Kristallographie, 137, 360–367.

Méring, J. (1975) Smectites. In J.E. Gieseking, Ed., Soil components, vol. 2, Inorganic components, p. 97–119. Springer, New York.

Pedro, G. (1974) Structure et réactivité des argiles. Bulletin du Groupe français des Argiles, 26, 9–55.

Radoslovich, E.W. (1963a) The cell dimensions and symmetry of layer-lattice silicates. IV. Interatomic forces. American Mineralogist, 48, 76–99.

——— (1963b) The cell dimensions and symmetry of layer-lattice silicates. V. Composition limits. American Mineralogist, 48, 348–367.

Radoslovich, E.W., and Norrish, K. (1962) The cell dimensions and symmetry of layer-lattice silicates. I. Some structural considerations. American Mineralogist, 47, 599–616.

Ross, M., Takeda, H., and Wones, D.R. (1966) Mica polytypes: systematic description and identification. Science, 151, 191–193.

Sanero, E. (1940) La struttura della xantofillite. Periodico di Mineralogia, Roma, 11, 53–88.

Schreyer, W., Abraham, K., and Kulke, H. (1980) Natural sodium phlogopite coexisting with potassium phlogopite and sodian aluminian talc in a metamorphic evaporite sequence from Derrag, Tell Atlas, Algeria. Contributions to Mineralogy and Petrology, 74, 223–233.

Shannon, R.D., and Prewitt, C.T. (1969) Effective ionic radii in oxides and fluorides. Acta Crystallographica, B 25, 925–946.

——— (1970) Revised values of effective ionic radii. Acta Crystallographica, B 26, 1046–1048.

Shirozu, H., and Bailey, S.W. (1966) Crystal structure of a two-layer Mg-vermiculite. American Mineralogist, 51, 1124–1143.

Sinno, R. (1952) Ricerche chimiche sui pirosseni del Somma-Vesuvio. Bollettino della Società dei Naturalisti in Napoli, 61, 77–82.

——— (1956) Confronto tra la composizione chimica del pirosseno del Vesuvio e quello dei Campi Flegrei. Bollettino della Società dei Naturalisti in Napoli, 65, 59–67.

Sunagawa, I., and Tomura, S. (1976) Twinnings in phlogopite. American Mineralogist, 61, 939–943.

Suquet, H., de la Calle, C., and Pézerat, H. (1975) Swelling and structural organization of saponite. Clays and Clay Minerals, 23, 1–9.

Suquet, H., Malard, C., and Pézerat, H. (1980) Etude du contenu en eau des saponites et vermiculites sodiques et calciques. Bulletin de Minéralogie, 103, 230–239.

Takeda, H. (1967) Determination of the layer stacking sequence of a new complex mica polytype: A 4-layer lithium fluorophlogopite. Acta Crystallographica, 22, 845–853.

Veitch, L.G., and Radoslovich, E.W. (1963) The cell dimensions and symmetry of layer-lattice silicates. III. Octahedral ordering. American Mineralogist, 48, 62–75.

Velde, B. (1971) The stability and natural occurrence of margarite. Mineralogical Magazine. 38, 317–323.

——— (1979) Cation-apical oxygen vibrations in mica tetrahedra. Bulletin de Minéralogie, 102, 33–34.

——— (1980) Cell dimensions, polymorph type, and infrared spectra of synthetic white micas: The importance of ordering. American Mineralogist, 65, 1277–1282.

Wearing, E. (1984) Platy phlogopite from blast-furnace slags. Mineralogical Magazine, 48, 81–84.

Ziebold, T.O., and Ogilvie, R.E. (1964) An empirical method for electron microanalysis. Analytical Chemistry, 36, 322–327.

Zvyagin, B.B., and Soboleva, S.V. (1979) Variabilité des longueurs de liaisons Si,Al_T–O dans les silicates lamellaires. Bulletin de Minéralogie, 102, 415–419.

Manuscript received February 20, 1986
Manuscript accepted January 17, 1987